J|A|C|S
ARTICLES

Layering at an Ionic Liquid−Vapor Interface: A Molecular Dynamics Simulation Study of [bmim][PF$_6$]

B. L. Bhargava and S. Balasubramanian*

Contribution from the Chemistry and Physics of Materials Unit, Jawaharlal Nehru Centre for Advanced Scientific Research, Jakkur, Bangalore 560 064, India

Received January 3, 2006; E-mail: bala@jncasr.ac.in

Abstract: The structure of the planar liquid−vapor interface of a room-temperature ionic liquid, 1-*n*-butyl-3-methylimidazolium hexafluorophosphate ([bmim][PF$_6$]), is studied using atomistic molecular dynamics simulations. Layering of the ions at the interface is observed as oscillations in the corresponding number density profiles. These oscillations, however, are diminished in amplitude in the electron density profile, due to a near cancellation in the contributions from the anions and the cations. An enhancement by 12% in the electron density at the interface over its value in the bulk liquid is observed, in excellent agreement with X-ray reflectivity experiments. The anions are found to predominantly contribute to this increase in the interfacial electron density. The cations present at the interface are oriented anisotropically. Their butyl chains are observed to be preferentially oriented along the interface normal and to project outside the liquid surface, thus imparting a hydrophobic character. In the densest region of the interface, the imidazolium ring plane is found to lie parallel to the surface normal, in agreement with direct recoil spectroscopy experiments.

---

1. Introduction

A new class of ionic salts, room-temperature ionic liquids (RTILs), is gaining widespread attention in industry and academia due to their interesting physical and chemical properties. These compounds, which are liquids at or around room temperature, have a negligibly low vapor pressure due to strong Coulombic interactions. They are thus termed “green solvents”, in contrast to traditional volatile organic solvents. RTILs are nonflammable, thermally stable, and liquid over a wide range of conditions, which makes them suitable for industrial applications.[1,2] Recent progress in environmentally friendly synthesis of these liquids is likely to make them even more viable.[3] Due to these possible potential applications, several experimental and computational studies of these compounds have been reported.[4−10] 1-*n*-Butyl-3-methylimidazolium hexafluorophosphate ([bmim][PF$_6$]) is one of the most studied RTILs. It has been used as a solvent and as a catalyst in several synthetic processes.[1,2,11,12] A number of computational studies have also been performed to understand the intermolecular structure and dynamics of this compound.[13−15]

Although the interface of a liquid with its vapor is small compared to its bulk, it plays a major role in many applications, such as multiphasic catalytic reactions, and hence its study is of primary importance.[1] Properties of liquids and ion concentrations at a liquid−vapor interface have been documented to be different than those in bulk.[16] In the case of RTILs, a number of experimental investigations have been carried out to determine the location and orientation of the ions at the air−ionic liquid interface.[17−22]

Neutron reflectivity studies[20] indicate a possible layering of molecules in liquid [bmim][BF$_4$] which extends up to 40 Å from the liquid−vapor interface. The ionic liquid−vapor interface has also been studied by using direct recoil spectroscopy (DRS)[18,19] and sum frequency generation (SFG) techniques.[21,23] While the SFG experiments conclude that the butyl tail of the cation points away from the surface with a certain tilt, DRS results indicate that the plane of the imidazolium ring is perpendicular to the surface and that the butyl tails are parallel

---

(1) Welton, T. *Chem. Rev.* **1999**, *99*, 2071.
(2) Earle, M. J.; Seddon, K. R. *Pure Appl. Chem.* **2000**, *72*, 1391.
(3) Wu, W.; Li, W.; Han, B.; Zhang, Z.; Jiang, T.; Liu, Z. *Green Chem.* **2005**, *7*, 701.
(4) Kanakubo, M.; Umecky, T.; Aizawa, T.; Kurata, Y. *Chem. Lett.* **2005**, *34*, 324.
(5) Hanke, C. G.; Price, S. L.; Lynden-Bell, R. M. *Mol. Phys.* **2001**, *99*, 801.
(6) Hanke, C. G.; Lynden-Bell, R. M. *J. Phys. Chem. B* **2003**, *107*, 10873.
(7) Del Popolo, M. G.; Voth, G. A. *J. Phys. Chem. B* **2004**, *108*, 1744.
(8) Yan, T.; Burnham, C. J.; Del Popolo, M. G.; Voth, G. A. *J. Phys. Chem. B* **2004**, *108*, 11877.
(9) Wang, Y.; Voth, G. A. *J. Am. Chem. Soc.* **2005**, *127*, 12192.
(10) Wang, Y.; Izvekov, S.; Yan, T.; Voth, G. A. *J. Phys. Chem. B* **2006**, *110*, 3564.
(11) Earle, M. J.; McCormac, P. B.; Seddon, K. R. *Green Chem.* **1999**, *1*, 23.
(12) Sheldon, R. *Chem. Commun.* **2001**, 2399.
(13) Margulis, C. J.; Stern, H. A.; Berne, B. J. *J. Phys. Chem. B* **2002**, *106*, 12017.
(14) Margulis, C. J. *Mol. Phys.* **2004**, *102*, 829.
(15) Huang, X.; Margulis, C. J.; Li, Y.; Berne, B. J. *J. Am. Chem. Soc.* **2005**, *127*, 17842.
(16) Jungwirth, P.; Tobias, D. J. *J. Phys. Chem. B* **2002**, *106*, 6361.
(17) Gannon, T. J.; Law, G.; Watson, P. R. *Langmuir* **1999**, *15*, 8429.
(18) Law, G.; Watson, P. R. *Chem. Phys. Lett.* **2001**, *345*, 1.
(19) Law, G.; Watson, P. R.; Carmichael, A. J.; Seddon, K. R. *Phys. Chem. Chem. Phys.* **2001**, *3*, 2879.
(20) Bowers, J.; Vergara-Gutierrez, M. C. *Langmuir* **2004**, *20*, 309.
(21) Iimori, T.; Iwahashi, T.; Ishii H.; Seki, K.; Ouchi, Y.; Ozawa, R.; Hamaguchi, H.; Kim, D. *Chem. Phys. Lett.* **2004**, *389*, 321.
(22) Sloutskin, E.; Ocko, B. M.; Tamam, L.; Kuzmenko, I.; Gog, T.; Deutsch, M. *J. Am. Chem. Soc.* **2005**, *127*, 7796. Sloutskin, E.; Ocko, B. M.; Tamam, L.; Kuzmenko, I.; Gog, T.; Deutsch, M. *J. Am. Chem. Soc.* **2005**, *127*, 18333.
(23) Sung, J.; Jeon, Y.; Kim, D.; Iwahashi, T.; Iimori, T.; Seki, K.; Ouchi, Y. *Chem. Phys. Lett.* **2005**, *406*, 495.

10.1021/ja060035k CCC: $33.50 © 2006 American Chemical Society

to the surface in liquid [bmim][PF_6] and perpendicular to it in [bmim][BF_4].[18,19] In recent SFG experiments, Rivera-Rubero and Baldelli[24] observed the butyl tail to project into the vapor phase and the ring plane to lie flat on the liquid surface. Obviously, there is a need to resolve these issues.

Deutsch and co-workers[22] have recently reported X-ray reflectivity and surface tension data for the [bmim][PF_6]−vapor interface. They observed a 10−12% increase in the density of electrons at the interface compared to that in the bulk, and they concluded that this interface does not exhibit density oscillations, such as those observed in liquid metals[25] or in the MD simulations of a [mmim][Cl]−vapor interface.[26,27] Very recent simulations of the liquid−vapor interfaces of [bmim][PF_6] and [bmim][BF_4][28] have also indicated oscillations in number and electronic densities, in apparent disagreement with the X-ray reflectivity experiments.

Our primary purpose is to try to resolve the apparent discrepancies between simulations and experiment on the nature of the electron density profile near the liquid−vapor interface of [bmim][PF_6]. Motivated by this aim, we present here results of fully atomistic molecular dynamics simulations of the liquid [bmim][PF_6]−vapor interface. Anticipating our results, we observe number density oscillations at the liquid−vapor interface in agreement with earlier simulations. However, the amplitude of the oscillations in the electron density profile is much less when compared to that in the number density profile, a feature that arises out of a near cancellation in the contribution to the former from the cations and the anions. This observation reconciles experiments and simulations. Further, we observe the liquid surface to possess a hydrophobic character.

We present details on the methodology and analyses employed in the next section, and discuss our results later.

2. Methodology and Simulation Details

Empirical potential molecular dynamics simulations were carried out on a planar liquid slab of 1-*n*-butyl-3-methylimidazolium hexafluorophosphate in equilibrium with its vapor. The simulations were carried out in the canonical ensemble using an all-atom model that was developed by Pádua and co-workers[29] to study crystal forms of ionic liquids. We have employed this potential to study the structure and dynamics of liquid [mmim][Cl][30] and have also employed it to generate initial configurations of an ab initio MD simulation[31] recently. Intramolecular interaction parameters for the $[PF_6]^-$ anion were adopted from the work of Borodin et al.,[32] making the model a fully flexible one. The current simulations were carried out on two different system sizes at three temperatures using the PINY_MD[33] code. System A consisted of 256 ion pairs (8192 atoms), while system B contained 512 ion pairs (16 384 atoms). The simulation of the latter, with twice the number of ions along the *z*-direction as that in system A, was necessary to obtain a truly bulk-like region in the center of the liquid slab. For system A, a pre-equilibrated bulk configuration (equilibrated for 8 ns) of 256 ion pairs within a cubic box of edge length 44.83 Å was placed at the center of a tetragonal supercell of dimensions 44.83 Å × 44.83 Å × 90.00 Å, so that two ionic liquid−vacuum interfaces were present in a supercell. A similar procedure of equilibration in bulk was adopted for system B, and the size of the supercell in the *z*-direction was chosen to be 150 Å for its interface calculations. Three-dimensional periodic boundary conditions were employed. The final configuration at each temperature was used as the starting configuration for the run at the subsequent lower temperature. Details on these simulations are summarized in Table 1. In addition to the above calculations, a second MD run, starting from an independent configuration of 512 ion pairs at 400 K, was quenched to 300 K. This system was equilibrated for 1.2 ns, and a subsequent trajectory of duration 2.5 ns was obtained for analyses. We label this as run C. Specifically, we obtained the mass and electron density profiles reported here as averages from runs B and C.

Table 1. Details of Simulated Systems

no. of ion pairs	temp (K)	supercell dimensions b_x, b_y, b_z (Å)	equilibration run length (ns)	analysis run length (ns)
256	500	44.83, 44.83, 90.00	6.0	4.8
256	400	44.83, 44.83, 90.00	1.2	6.1
256	300	44.83, 44.83, 90.00	1.2	14.8
512	500	44.83, 44.83, 150.00	3.0	2.0
512	400	44.83, 44.83, 150.00	1.2	2.2
B. 512	300	44.83, 44.83, 150.00	1.2	31.1
C. 512	300	44.83, 44.83, 150.00	1.2	2.5

The Ewald summation method with tinfoil boundary conditions was used for the computation of electrostatic interactions,[34] and α values of 0.265 and 0.268 $Å^{-1}$ were employed for systems A and B, respectively. A total of 8581 and 12 116 reciprocal vectors were used in the reciprocal space sum for the two systems, which guaranteed convergence of the Coulomb energy. A Nosé−Hoover chain thermostat[35] was used to control the temperature. The equations of motions were integrated using the reference system propagator algorithm (RESPA).[36] Nonbonded interactions within 13 Å (the interaction cutoff) and beyond 6 Å were integrated with a time step of 3 fs, and a 1.5 fs time step was used to integrate nonbonded interactions within 6 Å. Torsional forces were evaluated every 0.75 fs, and stretching and bending degrees of freedom were integrated with time steps of 0.375 fs. The conservation in total energy was 7 parts in 10^5 over 1 ns at 300 K.

In all the simulations carried out at 300, 400, and 500 K, none of the ions were found to be exclusively in the vapor phase, a consequence of the negligible vapor pressure of this liquid at these temperatures.

Configurations from the MD trajectory were stored every 0.9 ps during the analysis phase of the simulation. For the calculation of various density profiles, a bin width of 1 Å was used. At each instant, the center of mass of the system was translated to the origin before obtaining the profile. In some of the illustrations, the density profiles have been averaged over the two interfaces, where the *z*-component of the center of mass is taken as the zero along the *z*-axis. The electron density profile was calculated by considering the total number of electrons of each atom and subtracting the partial charge associated with that atom corresponding to the interaction potential employed here. The results were not dependent on whether one subtracted the site partial charges or not, indicating the robustness of the profiles obtained. While calculating the orientation of different vectors with respect to the surface normal (*z*-axis), the interfacial region is taken to be that up to the first

---

(24) Rivera-Rubero, S.; Baldelli, S. *J. Phys. Chem. B.* **2006**, *110*, 4756.
(25) Regan, M. J.; Pershan, P. S.; Magnussen, O. M.; Ocko, B. M.; Deutsch, M.; Berman, L. E. *Phys. Rev. B* **1996**, *54*, 9730.
(26) Lynden-Bell, R. M. *Mol. Phys.* **2003**, *101*, 2625.
(27) Lynden-Bell, R. M.; Kohanoff J.; Del Popolo, M. G. *Faraday Discuss.* **2005**, *129*, 57.
(28) Lynden-Bell, R. M.; Del Popolo, M. G. *Phys. Chem. Chem. Phys.* **2006**, *8*, 949.
(29) Lopes, J. N. C.; Deschamps, J.; Pádua, A. A. H. *J. Phys. Chem. B* **2004**, *108*, 2038. Lopes, J. N. C.; Deschamps, J.; Pádua, A. A. H. *J. Phys. Chem. B* **2004**, *108*, 11250.
(30) Bhargava, B. L.; Balasubramanian, S. *J. Chem. Phys.* **2005**, *123*, 144505.
(31) Bhargava, B. L.; Balasubramanian, S. *Chem. Phys. Lett.* **2006**, *417*, 486.
(32) Borodin, O.; Smith, G. D.; Jaffe, R. L. *J. Comput. Chem.* **2001**, *22*, 641.
(33) Tuckerman, M. E.; Yarne, D. A.; Samuelson, S. O.; Hughes, A. L.; Martyna, G. J. *Comput. Phys. Commun.* **2000**, *128*, 333.
(34) Allen, M. P.; Tildesley, D. J. *Computer Simulation of Liquids*; Clarendon Press: Oxford, 1987.
(35) Martyna, G. J.; Klein, M. L.; Tuckerman, M. E. *J. Chem. Phys.* **1992**, *97*, 2635.
(36) Tuckerman, M. E.; Berne, B. J.; Martyna, G. *J. Chem. Phys.* **1992**, *97*, 1990.

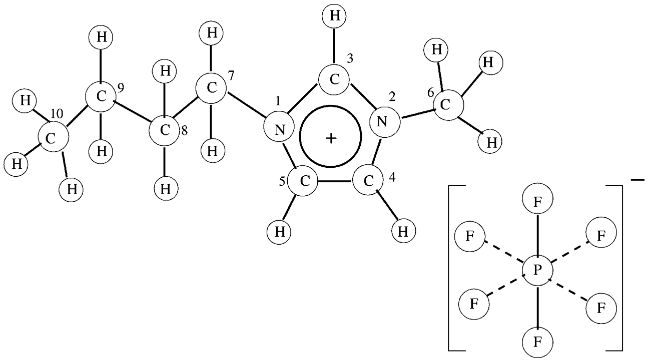

Figure 1. Schematic of [bmim][PF$_6$].

minimum in the mass density profile. The region between the center of mass and the first minimum is considered to be "bulk".

The surface tension γ was calculated using the diagonal components of the pressure tensor P_{ii}, employing the formula[37,38]

$$\gamma = -b_z(P_{xx} + P_{yy} - 2P_{zz})/4 \qquad (1)$$

where b_z is the length of the supercell in the direction parallel to the interface normal (z-axis), and the presence of the two equivalent interfaces is taken into account by introducing a factor of 2 in the denominator. The pressure tensor of the systems was stored every time step to calculate γ.

3. Results and Discussion

A schematic of the molecular structure of [bmim][PF$_6$] is presented in Figure 1 in order to aid the discussion.

3.1. Mass Density. Simulations of an open interface provide a good means to estimate the bulk density of a liquid. In Figure 2a, we show the mass density profile along the z-axis for the two simulated systems at 300 K. Note that the heights of the first peak on either interface of the larger system are comparable, signifying that the sample is well equilibrated. The mass density in the bulk region, estimated between $z = -38$ Å and $z = +38$ Å, of system B is 1.34 g/cm^3, which is within 1.5% of the experimental value of 1.36 g/cm^3.[39] The profiles from the two system sizes overlap with each other in the bulk region. The density oscillations are quite strong and are discernible even for a distance of 20 Å away from the interfaces. Figure 2b shows the symmetrized mass density profiles for the same system at the three temperatures. An expansion of the film with increasing temperature can be observed. The variation of the thickness (t) of the film in angstroms, with temperature T in Kelvin, can be expressed as $t = 35.5 + 0.03T$. The thermal expansion coefficient of the film between 300 and 500 K is obtained as 6.3×10^{-4} K^{-1}, which compares well with the experimentally determined value of 6.0×10^{-4} K^{-1}.[40]

3.2. Electron and Number Densities. X-ray reflectivity studies on interfaces probe the depth profile of electron density. As discussed earlier, Deutsch and co-workers have recently concluded that the electron density profile at a [bmim][PF$_6$]−vapor interface does not show oscillations.[22] To compare with these experiments, we show in Figure 3 the electron density profile along the z-axis for the 256 and 512 ion pair systems at 300 K. The first thing to note is that there is a non-negligible increase in the electron density near the interface as compared to that in the bulk.

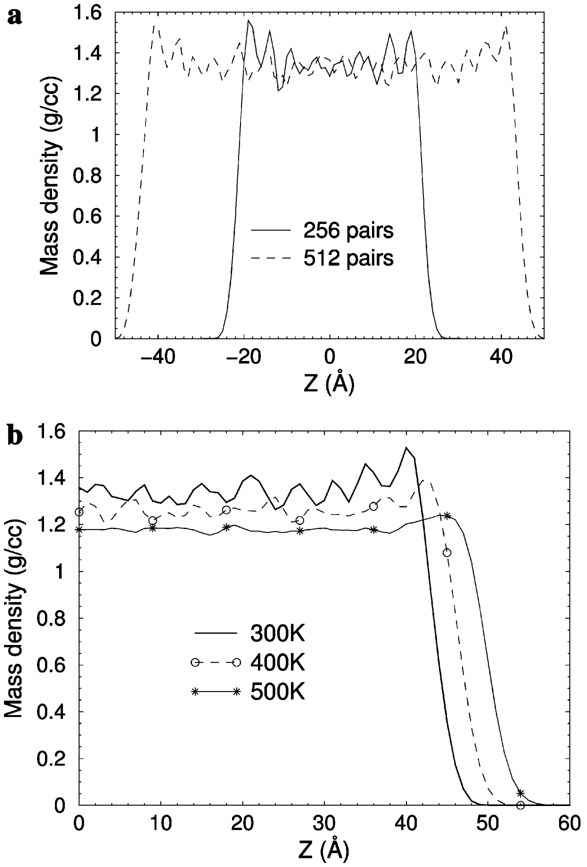

Figure 2. (a) Mass density profile along the z-axis for systems containing 256 and 512 ion pairs at 300 K. (b) Mass density profile along the z-axis for the 512 ion pair system at different temperatures.

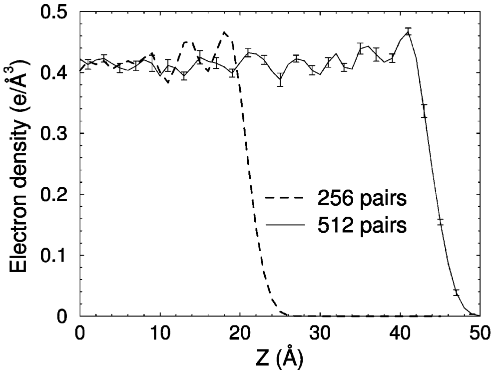

Figure 3. Electron density profile of 256 and 512 ion pair systems at 300 K.

Note that the peak height at the interface reaches a value of 0.47 e/Å^3, which is comparable to the interfacial electron density of 0.50 e/Å^3 obtained from experiments.[22] The average electron density in bulk for the 512 pair system at 300 K is 0.41 e/Å^3. Thus, the electron density at the interface is around 12% larger than that in bulk, a result that is consistent with the X-ray reflectivity studies, which measured a 10−12% increase.[22] The enhancement in electron density at the interface over the bulk value at temperatures of 400 and 500 K are around 9% and 5%, respectively. Thus, the density differentials decrease with

---

(37) Rao, M.; Berne, B. J. *Mol. Phys.* **1979**, *37*, 455.

(38) González-Melchor, M.; Bresme, F.; Alejandre, J. *J. Chem. Phys.* **2005**, *122*, 104710.

(39) Huddleston, J. G.; Visser, A. E.; Reichert, W. M.; Willauer, H. D.; Broker, G. A.; Rogers, R. D. *Green Chem.* **2001**, *3*, 156.

(40) Cadena, C.; Anthony, J. L.; Shah, J. K.; Morrow, T. I.; Brennecke, J. F.; Maginn, E. J. *J. Am. Chem. Soc.* **2004**, *126*, 5300.

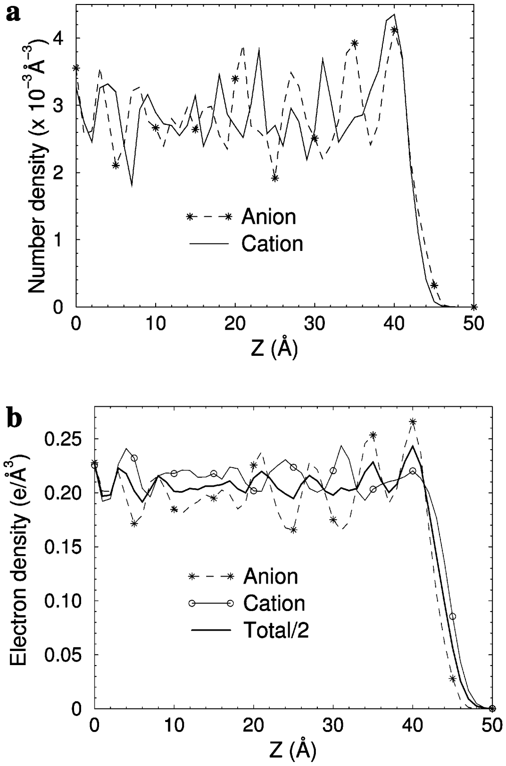

Figure 4. (a) Number density profiles of cations and anions for the 512 ion pair system at 300 K. (b) Profile of contributions from anions and cations to the total electron density.

increasing temperature, as expected. The amplitude of the oscillations also decreases with the increase in temperature, which is consistent with the observations of Lynden-Bell[26] on [mmim][Cl]. As we shall discuss later, the magnitude of such oscillations in the electron density profile in [bmim][PF_6] at 300 K is much diminished when compared to that found in the number density profiles of the cation and anion.

Shown in Figure 4a are the number density profiles of the cation and anion centers at 300 K from run B. In the case of the cation, this is defined to be the ring center, while the coordinate of the phosphorus atom is taken as the center of the anion. Pronounced oscillations and layering are observed for both the ions. Notwithstanding the oscillations seen in the number density profiles of the cation ring centers and that of the anions, what matters to the total electron density profile shown in Figure 3 are the individual contributions from these two species, which we study in Figure 4b. Here we show the contribution to the electron density profile obtained from the cations and from the anions separately. Their sum is the profile shown in Figure 3, which is reproduced also in Figure 4b for convenience. As expected from the behavior of the number density profiles, the electron density profiles of the cation and the anion exhibit oscillations. The positions of the first peak in the profiles of the ions in Figure 4b are similar. However, the positions of the second and subsequent peaks are out of phase. This behavior is clearly visible in the positions of the third and fourth peaks of the cation profile, which coincide exactly with the minima in the electron density profile of the anions. As a consequence, the amplitude of the oscillations in the total electron density profile is diminished compared to those in the individual partial electron density profiles. *This is our central result, which neatly relates the supposed absence of electron density oscillations in the experiments of Deutsch and co-workers[22] and the number density oscillations observed in our simulations as well as others.[26,28,41]*. Similar out-of-phase oscillations in the ion contributions to the electron density profile were observed in two other independent MD trajectories as well at 300 K for the 512 ion pair system. The cross correlation between these two contributions has been evaluated to be −0.54, averaged over three independent MD trajectories of the 512 ion pair system at 300 K. Values of +1 and −1 would mean fully correlated and fully anti-correlated functions, respectively. Thus, the result of −0.54 obtained here quantifies our observation of out-of-phase oscillations in the anion and cation contributions, as exemplified in Figure 4b.

The anion is found to be mainly responsible for the enhancement of the electron density at the interface, as can be seen in Figure 4b. Although the number density profile for the cation shows a marginally taller peak at the interface compared to that of the anion (see Figure 4a), the contribution from the cation to the total electron density is nearly uniform, with few oscillations, whose amplitudes are smaller than those present in the anion contribution. This result can be rationalized on the basis of the higher molecular volume of the cation, which results in its electron cloud being more distributed. The anion contribution to the total electron density profile mirrors its number density profile. The combination of these two factors leads to oscillations in the total electron density.

An enhancement in the molar fraction of the anions at the interface was predicted by Deutsch and co-workers,[22] as anions are the only electron-rich species which could account for the observed interfacial electron density of 0.5 e/Å^3. It turns out from our data that the anions' contribution to the electron density enhancement is substantially larger than that of the cations. However, this fact does not necessarily imply that the anion number density at the interface has to be larger than that of the cation. Our observations indicate that the interpretation of the reflectivity experiments is nuanced. An increase in the interfacial electron density need not preclude an increase in the number density of cations at the interface over the bulk value. In addition, as stated earlier, the decreased amplitude of oscillations in the total electron density profile can be consistent with the presence of strong oscillations in the number density of ions.

3.3. Orientation of Cation. Having reconciled this apparent disagreement between experiment and simulations, we proceed now to examine other properties of the interface. We study the orientation of the butyl tail for cations which are present at the interface. In Figure 5a, we present the distribution of the angle between the butyl chain (i.e., the N1−C10 vector) and the surface normal (*z*-axis).

We observe that the most probable orientation of the butyl chain is parallel to the surface normal. Thus, the outermost part of the surface of [bmim][PF_6] liquid is constituted by the butyl chains of the cation, and hence the surface should possess some degree of hydrophobic character. At 300 K, a significant number of butyl chains possess a gauche defect in the central C−C bond. However, we have found that the percentage of such defects is only marginally increased for cations present at the interface when compared to those in bulk (data not shown). We have also studied the orientation of the cation ring with respect to

---

(41) Yan, T.; Li, S.; Jiang, W.; Gao, X.; Xiang, B.; Voth, G. A. *J. Phys. Chem. B.* **2006**, *110*, 1800.

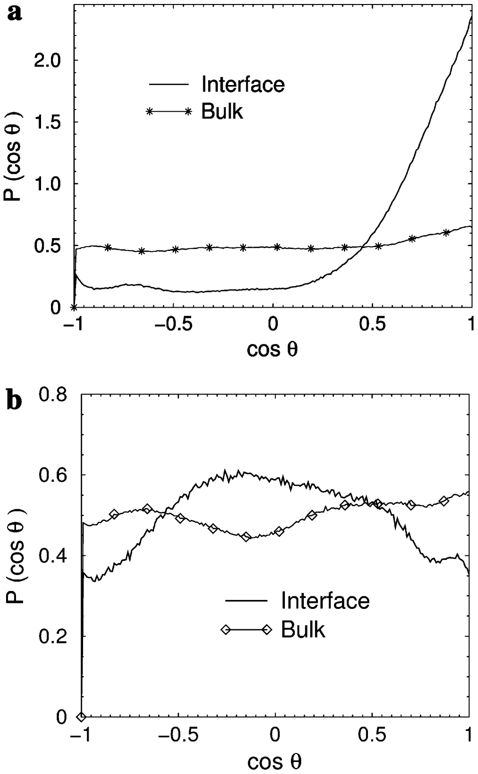

Figure 5. (a) Orientation of the chain vector with respect to the interface normal (*z*-axis) in the interfacial and bulk regions. θ is the angle between the vector N1−C10 and the *z*-axis. (b) Orientation of the ring normal with respect to the interface normal (*z*-axis) in the interfacial and bulk regions. θ is the angle between the normal to the imidazolium ring plane and the *z*-axis.

the surface normal. In Figure 5b, we show the probability distribution for the angle between the ring normal and *z*-axis. At the interface, there is a marked preference for the N−N vector of the cation to be parallel to the surface normal (*z*-axis), a result that is consistent with direct recoil spectrometry data.[17] However, these distributions are rather wide, and hence preferences for orientations are not very strong. Further, the liquid surface is rough at the length scales of a few angstroms, and hence preferences for specific orientations obtained from such distributions should not be used to build molecular cartoons of the surface in which structural motifs other than the preferred ones are absent.

Figure 6 summarizes the interfacial structure. The terminal methyl group of the butyl chain is present in the outermost part of the interface, followed by the nitrogen atom (N1) to which the butyl chain is attached, the anion, the center of the imidazolium ring, the nitrogen atom to which the methyl group is attached (N2), and then the methyl group attached to the ring. A surface alignment of the cation is evident, with the most probable orientation being that where the butyl chains are aligned parallel to the surface normal. The butyl tails of the cations at the interface are interspersed by the anions.

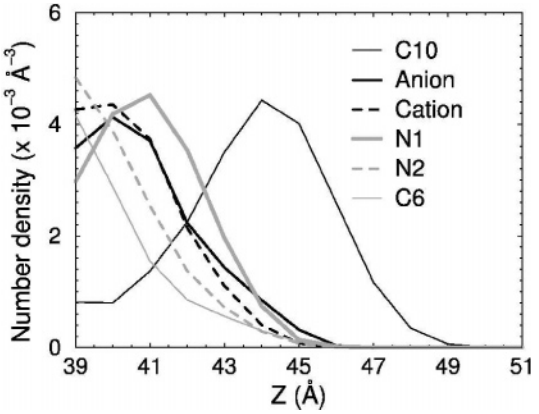

Figure 6. Number density profile of different sites on the cation and the anion at 300 K for the 512 ion pair system.

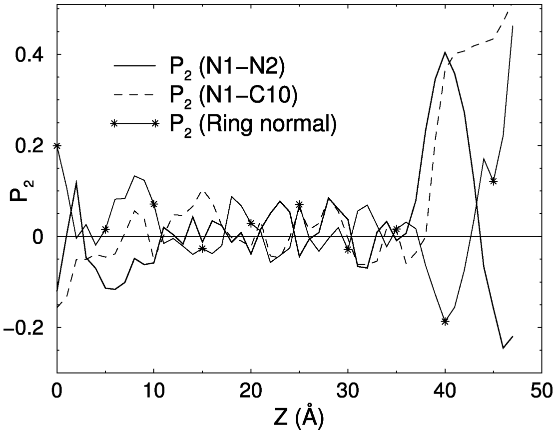

Figure 7. Averages $\langle P_2(\cos\theta)\rangle$ of the angle between the specified vector and the surface normal for the 512 ion pair system at 300 K.

The orientation of the cations in the system can be described by Legendre polynomials, which are defined as $P_1(\cos\theta) = \cos\theta$ and $P_2(\cos\theta) = (1/2)(3\cos^2\theta - 1)$. Such functions enable us to obtain an idea of the range and extent of orientational preferences at the interface. The averages $\langle P_2(\cos\theta)\rangle$ for the NN vector, the butyl vector of the cation, and the normal to the imidazolium ring with respect to the *z*-axis are shown in Figure 7. The peak value for the butyl chain function at the interface is in the range of 0.4−0.5, which indicates the degree of orientational preference, relative to a value of unity expected for perfect ordering. The position dependence of the orientation of the N−N vector (i.e., the ring plane) with respect to the surface normal is interesting. Between $z = 43$ Å and $z = 46$ Å, the value of its P_2 function is negative, implying that the ring plane is flat on the surface. This can also be seen from Figure 6, where beyond $z = 45$ Å, the number density profiles of N1, N2, and the cation (center of the ring), which determine the plane of the ring, almost coincide, which is a clear indication of the ring being aligned nearly parallel to the surface. Beneath this exposed surface lies a high-density region in which the ring plane of the cation is perpendicular to the plane of the interface. This might explain the differences observed in the cation ring orientation between SFG[24,42] and DRS experiments.[18,19] The former observe the ring plane to be flat on the surface, while the latter report a perpendicular orientation. It should be noted, however, that the range of such an orientational preference is rather short, with only the first layer at the surface exhibiting such preferences. In the bulk region, the second-order Legendre polynomial for all the angles vanishes due to its isotropicity, as expected.

The surface tension values for the 256 ion pair system were estimated to be 73, 38, and 36 mN m^{-1} at temperatures of 300, 400, and 500 K, respectively. The value at 300 K is larger than the experimental value of 45 mN m^{-1}.[22,43] The difference could

---

(42) Rivera-Rubero, S.; Baldelli, S. *J. Am. Chem. Soc.* **2004**, *126*, 11788.

point to deficiencies in the model potential as well as to the smaller surface area employable in simulations compared to experiments. Surface tension is a rather tough quantity to converge in equilibrium simulations. For instance, at 300 K, the estimated standard deviation on the mean value of 73 mN m^{-1} is 222 mN m^{-1}! Nonequilibrium methods to obtain surface tension from atomistic simulations could be helpful.

4. Conclusions

The microscopic structure of the liquid [bmim][PF_6]−vapor interface has been elucidated using atomistic molecular dynamics simulations. The potential model is found to predict the bulk density and thermal expansion coefficient of the liquid quite well, although the calculated surface tension is larger than the experimental value. We summarize our main results as follows.

(i) Density oscillations are observed at the interface — in the number density of cations and anions, in the mass density, and also in the electron density. Oscillations in the electron density are much diminished when compared to the amplitude of oscillations in the number densities, due to a near cancellation in the contribution from the anions and that of the cations.

(ii) The electron density at the interface is around 12% larger than that in the bulk. This result is in excellent agreement with conclusions drawn from X-ray reflectivity measurements.[22]

(iii) The enhanced electron density at the interface is largely contributed by the anions, although both anions and cations enrich the surface. The cationic contribution to the electron density profile is nearly featureless, due mainly to its larger molecular volume.

(iv) The butyl chain of the cations present at the interface exhibits a preference to orient along the surface normal. Hence, the surface could be expected to have a certain amount of hydrophobic character. However, the hydrophobicity of this surface will be less than that of a *n*-alkane, due to the presence of charged groups in the vicinity.

(v) In the densest region of the interface, the cation ring plane is oriented parallel to the surface normal. Closer to the vapor phase, which is rarer, the ring plane is parallel to the surface plane.

Our estimates of surface tension tend to be larger than the experimental value. Could the density oscillations observed here be related to the higher surface tension of the simulated interface? We discount this possibility, as such oscillations are observed in our systems at 400 and 500 K as well, where our surface tension estimates are comparable to the experimental value (at 300 K). This provides us confidence that density oscillations are indeed present in liquid [bmim][PF_6] at its vapor interface at 300 K. However, simulations study much smaller samples than considered in experiments, and hence they do not include effects of capillary waves.

The observation of large-amplitude oscillations in the number density at the interface is in apparent disagreement with the conclusions from X-ray reflectivity experiments.[22] The electron density profile obtained here exhibits oscillations with the same period as one of the profiles reported by Deutsch et al., which was not selected for further analyses by them based on considerations of experimental resolution. On the other hand, in partial agreement with them, we find that the oscillations in the total electron density profile are diminished in amplitude relative to those found in the number density profile. The underlying reason for the observation of strong oscillations at the interface in the number densities of ions and weak ones in the electron density profile is the difference in the molecular sizes of the two species, being appropriate to nearly cancel out their contributions to the total electron density. This central result is unlikely to change with the inclusion of polarizable interactions. Recent MD simulations on the liquid−vapor interface of a different IL, i.e., [emim][NO_3], at 400 K[41] using a polarizable model exhibit similar features of an out-of-phase oscillation in the number densities of cations and anions, a result that is crucial to the arguments enunciated in our work. Such a behavior in the number density profile can lead to similar effects in the contribution of ions to the total electron density profile, as reported here. It thus appears that our interpretation of the decreased amplitude in the electron density profiles of the liquid−vapor interfaces of ionic liquids possessing short side chains could be general.

Acknowledgment. The research work reported here is supported by grants from the Department of Science and Technology, India. B.L.B. thanks CSIR, India, for a research fellowship.

JA060035K

---

(43) Law, G.; Watson, P. R. *Langmuir* **2001**, *17*, 6138.